

RSC Advances



This is an *Accepted Manuscript*, which has been through the Royal Society of Chemistry peer review process and has been accepted for publication.

Accepted Manuscripts are published online shortly after acceptance, before technical editing, formatting and proof reading. Using this free service, authors can make their results available to the community, in citable form, before we publish the edited article. This *Accepted Manuscript* will be replaced by the edited, formatted and paginated article as soon as this is available.

You can find more information about *Accepted Manuscripts* in the [Information for Authors](#).

Please note that technical editing may introduce minor changes to the text and/or graphics, which may alter content. The journal's standard [Terms & Conditions](#) and the [Ethical guidelines](#) still apply. In no event shall the Royal Society of Chemistry be held responsible for any errors or omissions in this *Accepted Manuscript* or any consequences arising from the use of any information it contains.

Manuscript for RSC Advance

A dual-fluorescent whole-well imaging approach for screening active compounds against doxorubicin-induced cardiotoxicity from natural products

Yaqi Chen¹, Lijuan Sun¹, Yi Wang^{1,*}, Xiaoping Zhao^{2,*}

(1) College of Pharmaceutical Sciences, Zhejiang University, Hangzhou 310058, PR China

(2) College of Preclinical Medicine, Zhejiang Chinese Medical University, Hangzhou 310053, PR China

***Corresponding author:** Yi Wang (mysky@zju.edu.cn), College of Pharmaceutical Sciences, Zhejiang University

Tel.: +86-571-88208426; fax: +86-571-88208426.

Xiaoping Zhao (zhaoxiaoping@zjtcu.net), College of Preclinical Medicine, Zhejiang Chinese Medical University.

Abstract

Doxorubicin (DOX) is an effective chemotherapy drug for various types of cancer. However, acute and chronic cardiotoxicity of DOX hamper its clinical application. There is a great demand for the discovery of drugs against DOX-induced cardiotoxicity. There is a great demand for the discovery of drugs against DOX-induced cardiotoxicity. This paper proposed a dual fluorescence cellular imaging assay for screening active compounds against DOX toxicity. Whole-well fluorescence images of cells in 96-well microplates were automatically acquired and reconstructed by using a fluorescence microscope coupled with a computer-controlled moving stage. DOX-injured cardiomyocytes were labeled with two fluorescent probes, namely, fluorescein diacetate and Hoechst 33342, to determine cell viability and apoptosis. The linear range and sensitivity of the proposed approach were evaluated and validated by a known active compound, rutin. The proposed approach was also successfully applied in screening active compounds from a clinically used herbal medicine **ZhenQiFuZheng granule (ZQFZ)**, which consisted of two herbs, *Astragalus membranaceus* (Fisch.) Bunge and *Ligustrum lucidum*. Five active components were found and were further analyzed by liquid chromatography coupled with mass spectrometry. Hydroxytyrosol, neoneuzhenide, salidroside, and cimidahurinine attenuated DOX-induced cardiotoxicity in a dose-dependent manner with EC_{50} values of 198.0, 260.4, 621.7, and 45.79 μM , respectively. Western blot results indicated that these active compounds protected against cardiotoxicity by decreasing reactive oxygen species (ROS) accumulation and downregulating apoptosis-related Bax/Bcl-2 proteins. The proposed approach is efficient for screening active compounds from natural products and other complex mixtures.

Keywords: High-content screening; Traditional Chinese medicine; Fluorescent microscopy; Cardiotoxicity

1. Introduction

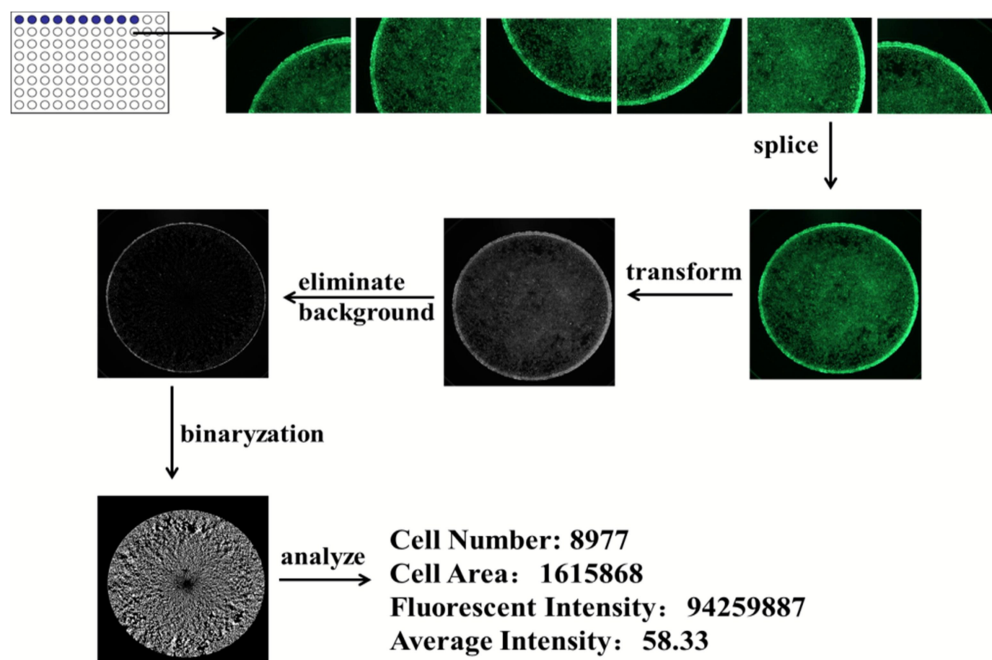
Fluorescence microscopy has been widely used in biomedicine to generate digital imaging data from living or fixed cells. Several automated fluorescence platforms have been developed and successfully applied in RNAi screening ¹, and high-content/throughput drug screening ². High-magnification fluorescence microscopy is commonly used to monitor intracellular phenomena and individual cell phenotypes, whereas low-resolution mode is used to detect changes in cell number or shape. However, 96- or 384-well microplate-based screening can only record representative images of four or eight positions in each well were; hence, the general phenotype of whole cell population could be lost. Ramirez et al ³ showed that whole-well imaging is more robust and sensitive than multi-tile imaging in screening reversers of a specific oncogene. Commercially available instruments for whole-well imaging are usually equipped with a large-chip CCD camera or expensive confocal microscope ⁴. In our preliminary efforts, we developed an automated high-throughput imaging assay that adopted a self-designed FluoinsightCell platform to detect single fluorescence labeling in hepatic and myocardiocyte cells ^{5,6} and screen hepatotoxic or cardioprotective compounds. The platform is consisted of an inverted fluorescence microscope, a pinpoint-accuracy moving stage, a charge-coupled device camera, and an image acquirement and recognizing system that controls the movement of stage and automatic focusing. Fluorescence images captured by FluoinsightCell can be processed by software to obtain useful information like fluorescence intensity. However, assays for the multiplex detection of cellular events at the whole-well level are still lacking. Therefore, the development of novel assays that simultaneously detect and quantify dual or triple fluorescence signals of cellular phenotype under various pathological or pharmacological environments is indispensable.

Doxorubicin (DOX) is a widely used chemotherapy drug for breast and oesophageal carcinomas, childhood solid tumors, and soft tissue sarcomas ⁷. However, the usage of DOX is hampered by its severe cardiotoxicity, including acute myocardial injury in the form of acute tachyarrhythmia and chronic cardiotoxicity induced heart failure and death ^{8,9}. Previous studies hypothesized that DOX induced cardiotoxicity by increasing cardiac oxidative stress and DNA intercalation/binding ¹⁰; inducing abnormalities in the mitochondria ¹¹; decreasing the activities of Na⁺, K⁺-adenosine triphosphatase (ATPase), and Ca²⁺-ATPase ^{12, 13}; And facilitating caspase activation-induced apoptosis in myocardial cells ¹⁴. A recent review concluded that oxidative stress and apoptosis are the main mechanisms associated with DOX-induced cardiotoxicity ¹⁵.

In the past decade, drugs that protect against DOX-induced toxicity have been developed. Those drugs include dexrazoxane, monoHER, beta-adrenergic antagonists and angiotensin converting enzyme (ACE) inhibitor. Naturally derived compounds such as isorhamnetin and rutin also reportedly protect DOX-injured cardiomyocytes

both *in vitro* and *in vivo*^{16, 17}. Therefore, herbal medicine and other natural products could be an invaluable resource for the discovery of DOX antagonists.

The present study aims to establish a dual-fluorescence imaging-based platform to screen active compounds against DOX-induced cardiotoxicity. The representative flowchart of the proposed methods is illustrated in Fig.1. In brief, fractions of natural products were prepared through standard isolation procedures. H9c2 cells were pre-incubated with these fractions, and then exposed to DOX. After dual staining with fluorescent probes, fluorescence images of H9c2 cells in each well were acquired and quantitatively analyzed to identify compounds that protect against DOX-induced injury. The linear range and sensitivity of the proposed approach were validated using positive controls. The proposed approach was applied in screening active compounds of ZhenQiFuZheng granule (ZQFZ), a marketed botanical drug that served as an immunopotentiator for cancer chemotherapy. Clinical observations showed that ZQFZ can improve the quality of life of patients with gastrointestinal neoplasms or ovarian cancer and reduce the adverse effect of chemotherapy^{18, 19}. Combined treatment of DOX and ZQFZ can also reduce DOX-induced adverse effects by decreasing plasma CK-MB and cTnI levels and recovering cardiac function in cancer patients²⁰. In this study, four active compounds were identified from ZQFZ while anti-apoptosis mechanism of two compounds was further investigated.



Scheme 1 Representative flowchart of automated imaging acquisition and processing by FluoinSightCell platform

2.Experimental

2.1. Reagents and materials

Fluorescein diacetate (FDA) and Hoechst 33342 obtained from Sigma Inc. (St. Louis, MO) were dissolved in dimethyl sulphoxide (Sigma, St. Louis, MO) and stored at -20°C until use. Doxorubicin hydrochloride was purchased from the National Institute for Food and Drug Control (Beijing, China). Cell culture reagents, including Dulbecco's modified Eagle's medium (DMEM), fetal bovine serum (FBS), and antibiotics were purchased from Gibco (Grand Island, NY). The standard chemicals of rutin were purchased from Shanghai Winherb Medical Technology Co. Ltd (Shanghai, China). HPLC-grade acetonitrile (Fisher, NJ, USA), formic acid (MERDA, USA) and ultrapure water (Milli-Q Plus, Millipore Co., Ltd., USA) were used in all experiments. All other chemicals and solvents are of analytical grade. ZhenQiFuZheng granules, a clinically used complementary drug for chemotherapy were obtained from Xiuzheng Pharmaceutical Group (China). ZQFZ fractions were prepared using standard procedures as illustrated in Electronic Supplementary Information (ESI) S1.

2.2. Cell culture

H9c2 cells were obtained from the Shanghai Cell Bank (Institute of Cell Biology, China Academy of Sciences, Shanghai, China). Cells were maintained in DMEM supplemented with 10% FBS and antibiotics ($100\text{U}\cdot\text{mL}^{-1}$ penicillin and $100\mu\text{g}\cdot\text{mL}^{-1}$ streptomycin) in a humidified atmosphere of 5% CO_2 at 37°C . When cell populations reached 70% to 80%, the cells were trypsinized and dispensed into 96-well plates.

2.3. Dual Fluorescence Assay using FluoinsightCell platform

The FluoinsightCell platform has been described in our previous report ⁶. As shown in Scheme.1, a specific well in a 96-well plate was divided into six parts to obtain six independent images using the microscope ($2.5\times$ objective, $20\times$ eyepiece). These images were then spliced into a whole-well image. The whole-well image was transformed to a grey image and then binarized after eliminating the fluorescence background. Useful information including cell number, cell area, fluorescence intensity, and average fluorescence intensity was generated. Therefore, the whole-well fluorescence images of selected wells in a standard 96-well microplate can be automatically acquired and analyzed.

Cardiomyocytes were stained with $10\mu\text{g}\cdot\text{mL}^{-1}$ FDA and/or Hoechst by adding the dye(s) into the cell media before incubating for 10 min. The cells were washed with PBS, and the cellular images were captured by the FluoinsightCell platform. To validate whether or not mono-staining and dual staining have similar results for each dye, the cells were dispensed into three plates at a density of 4000 cells per well for 24 h. Then, the cells were treated with different concentrations of DOX (0.01, 0.1, 0.3, 0.5, and $1.2\mu\text{M}$) for 24 h. Two plates mono-stained by FDA or Hoechst were compared with another plate with dual staining.

2.4. Sensitivity and linear range of the proposed approach

H9c2 was seeded into 96-well plates with different cell densities (0, 100, 500, 1000, 2000, 4000, 6000, 8000, and 10000 cells per well) for 24, 48, and 72 h. The cells were stained by FDA or Hoechst. The relationship between cell number and fluorescence intensity was evaluated. To select the optimal condition of DOX-induced cardiotoxicity, cells were exposed to various DOX concentrations (0.001 to 100 μM) for 24 h. Dexrazoxane, the only FDA-approved DOX antagonist, was also used to pre-incubate cells before DOX-induced injury.

2.5. Application to ZhenQiFuZheng granule

2.5.1 Screening of cardio protective components from ZQFZ granules

H9c2 cells were dispensed into 96-well plates at a density of $4 \times 10^4 \cdot \text{mL}^{-1}$. Test samples from ZQFZ were added to plates 30min before DOX treatment. Cardio protective effects of tested samples in each well of a microtiter plate were calculated using the following equations:

$$\text{Anti-viability damage (FDA fluorescence)} = \frac{\text{Sample-Dox treated}}{\text{Media control-Dox treated}}$$

$$\text{Anti-DNA damage (Hoechst fluorescence)} = \frac{\text{Sample-Dox treated}}{\text{Media control-Dox treated}}$$

where “media control” represents untreated cells, “DOX treated” represents fluorescence intensity collected from cells exposed to 0.3 μM DOX; “Sample” represents cells pre-incubated with tested samples (sample) and then exposed to DOX. In primary screening, the concentration of 52 tested fractions isolated from ZQFZ was set as 50 $\mu\text{g} \cdot \text{mL}^{-1}$ (unless fractions with cytotoxicity). In secondary screening, active fractions with significant activity for either anti-membrane damage or anti-DNA damage were selected out to validate their effects from 3.125 to 100 $\mu\text{g} \cdot \text{mL}^{-1}$. Finally, several identified active compounds were obtained to test their efficacy from 10 μM to 100 μM . The EC_{50} of active fractions and compounds was calculated by Graph Pad Prism 6.0 (GraphPad Software, Inc.).

2.5.2 Identification of cardioprotective compounds from ZQFZ

Cardioprotective fractions were dissolved in 500 μL of methanol–water. After centrifugation at 13,400 rpm for 5min, the supernatant was analyzed using a Triple TOF-TM 5600⁺ high-resolution mass spectrometer to determine the accurate molecular weight of compounds. The acquisition parameters for LC/ESI-MS were as follows: temperature, 600°C(-)/550°C (+); ionspray voltage floating, -4500 V/+5500 V; declustering potential, -100 V/+100 V; collision energy, -10 V/+10 V; ion source GS1,60 psi; ion source GS2, 60 psi; curtain gas, 25 psi; ma

range, m/z 100 to 1500. Chromatographic separation was carried out on a reversed-phase Zorbax SB-C₁₈ analytical column (250 mm × 4.6 mm I.D., 5 μm, Agilent Technologies, USA). The mobile phase consisted of water containing 0.05% (v/v) formic acid (A) and acetonitrile (B). A gradient program was used in accordance with the following profile: 0 min, 5% B; 5 min, 5% B; 25 min, 20% B; 50min, 30% B; 60min, 50% B; 63 min, 95% B; 68 min, 95% B; analysis time, 68 min. The flow rate was 0.6 mL·min⁻¹, the column temperature was 30°C, and the injection volume was 10 μL.

2.5.3 Western Blot

To investigate the mechanism by which hydroxytyrosol, neonuezhenide, salidroside and cimidahurinine exerts their cardioprotective effects, we examined Bcl-2 and Bax protein levels regulated by hydroxytyrosol, neonuezhenide, salidroside and cimidahurinine in DOX-injured primary cultured neonatal cardiomyocytes. Briefly, after being primary cultured for 72 h, neonatal cardiomyocytes were seeded into dishes. Rutin (100 μM), hydroxytyrosol (80 μM), neonuezhenide (50 μM), salidroside (100 μM) and cimidahurinine (60 μM) were added to cells for 30 min pre-incubation prior to treatment of 1 μM DOX for 24 h. The cells were lysed to obtain the protein extracts. The concentration of total protein was measured by BCA assay kit. Protein samples were mixed with loading buffer and reducing agent, then separated by 10% Bis-Tris gel, and then blotted on a PVDF membrane. The membrane was blocked in blocking buffer (5% bovine serum albumin) and incubated overnight with primary antibody of Bcl-2 (1:1000 in blocking buffer, Cell Signaling Technology), Bax (1:1000 in blocking buffer, Cell Signaling Technology). The membrane was washed thrice and then incubated with HRP anti-rabbit IgG for 1h at room temperature. ECL chemiluminescence reagent was used to visualize blots. The bands were exposed by Bio-Rad ChemiDoc XRS.

2.5.4 Intracellular ROS determination and Annexin V/PI dual staining

Intracellular ROS formation was measured by using a ROS assay kit (Beyotime). H9c2 cells were dispersed into 96-well plates at a density of 4×10⁴·mL⁻¹. After 24 h incubation, rutin (100 μM), hydroxytyrosol (100 μM), neonuezhenide (100 μM), salidroside (100 μM), and cimidahurinine (50 μM) were added to cells for 30min pre-incubation prior to treatment of DOX (0.3 μM) for 24 h. Then cells were washed with PBS and incubated with DCFH-DA (5 μM) for 30 min at 37 °C. After being washed twice with PBS, the DCF fluorescence of cells was detected by microplate reader spectrophotometer (Molecular Devices, America) with the parameters: excitation wavelength 488 nm, emission wavelength 525 nm.

Annexin V/PI dual staining was performed to prove the cardioprotective effect of hydroxytyrosol, neonuezhenide, salidroside, and cimidahurinine by using FITC Annexin V Apoptosis Detection Kit (BD). H9c2 cells were dispensed into dishes at a density of $2 \times 10^5 \cdot \text{mL}^{-1}$ for 24 h incubation. Hydroxytyrosol (80 μM), neonuezhenide (50 μM), salidroside (100 μM) and cimidahurinine (60 μM) were added to cells for 30 minutes pre-incubation prior to treatment of 1 μM DOX for 8 h. Then cells were harvested, washed with cold PBS twice and suspended in binding buffer. Annexin V-FITC (5 μL) and propidium iodide (5 μL) was added to each cell sample. The cells were analyzed by flow cytometry (Beckman Coulter).

2.6 Data analysis

All curves and columns were represented as the mean \pm SEM of three replicates. Differences in means among groups were tested by one-way ANOVA with Dunnett's test. Statistical significance was considered at $P < 0.05$. All statistical analyses were performed using GraphPad Prism (SPSS Inc., Chicago, IL).

3. Results and discussion

3.1. Sensitivity and linear range of dual fluorescence imaging approach

FDA is a positive nonpolar ester for detecting viable cells and can easily pass through cell membranes. After being hydrolysed by free exoenzymes and membrane-bound enzymes, fluorescein was released and remained in the undamaged membrane. Hoechst 33342, which combines with DNA, is commonly used to analyze DNA content and indicate cell apoptosis.

We investigated the relationship between cell number and fluorescence intensity for two fluorescent probes. FDA or Hoechst staining showed a linear relationship with cell number from 0 to 10,000 ($r^2 > 0.9$, Fig. 1a and 1b) for 24, 48, and 72 h. DOX dose-dependently induced cardiotoxicity in different cell densities (Fig. 1c, Fig. 1d).

The results of mono staining and dual staining were compared to evaluate whether fluorescence interference of two dyes exists. As shown in Fig. 2, the IC_{50} values of mono and dual staining with Hoechst were 0.23 and 0.17 μM , whereas those of mono or dual staining with FDA were 1.1 and 0.82 μM . The results indicated that the two experiments did not significantly differ. Therefore, the proposed method was sensitive with a satisfied linearity range.

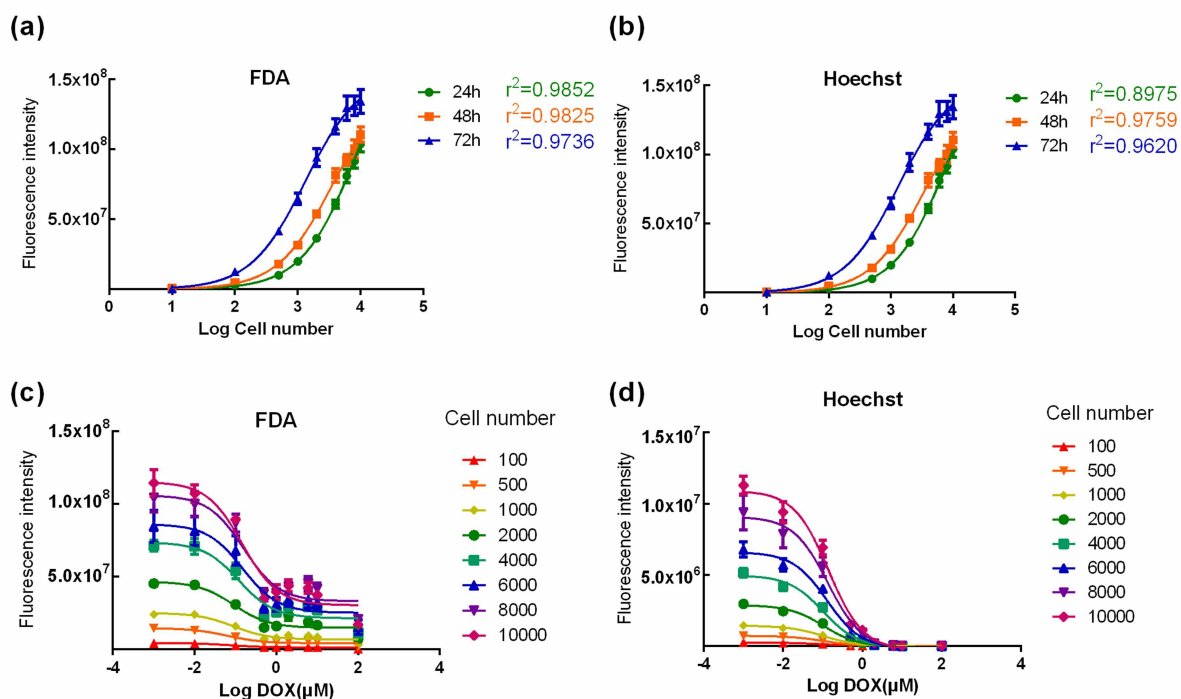


Fig. 1 Relationship between cell number and fluorescence intensity after FDA (A) or Hoechst(B) staining. Relationship between DOX concentration and the fluorescence intensity of injured H9c2 cells when stained by FDA (C) or Hoechst (D).

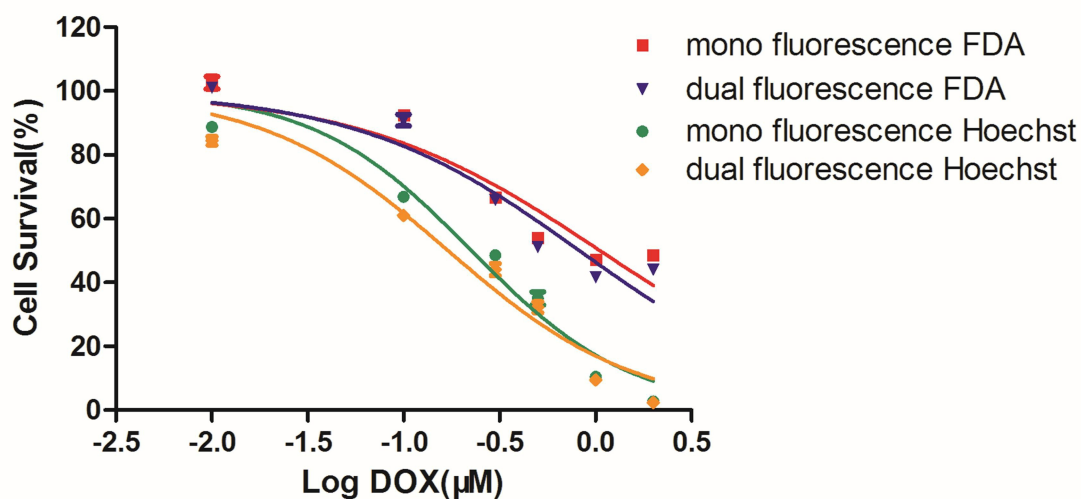


Fig. 2 Comparison of DOX-induced cardiotoxicity by mono and dual staining assay .

3.2. Validation of dual fluorescence imaging approach by rutin and dexrazoxane

Images of the cells pre-incubated with rutin (100 μM) and dexrazoxane (150 μM) and then treated with DOX were captured to observe the changes in cell viability and nucleus via FDA and Hoechst staining. As shown in Fig.3, the cell viability and nucleus of the cardiomyocytes were impaired by DOX. Pre-incubation with rutin and dexrazoxane can significantly increase the fluorescence intensity of the DOX-injured cells. The cells pretreated with 150 μM dexrazoxane showed approximately 20% cardio protective activity after DOX exposure on FDA-stained H9c2. This result agrees with previous results²¹. However, the cells treated with dexrazoxane displayed an approximately 9% increase in Hoechst fluorescence. This finding suggests that the protective effect of dexrazoxane is chiefly attributed to preventing cellular membrane impairment rather than DNA damage. Consistent with this finding, a previous study reported that dexrazoxane can decrease free radicals through iron chelation by its hydrolysates²².

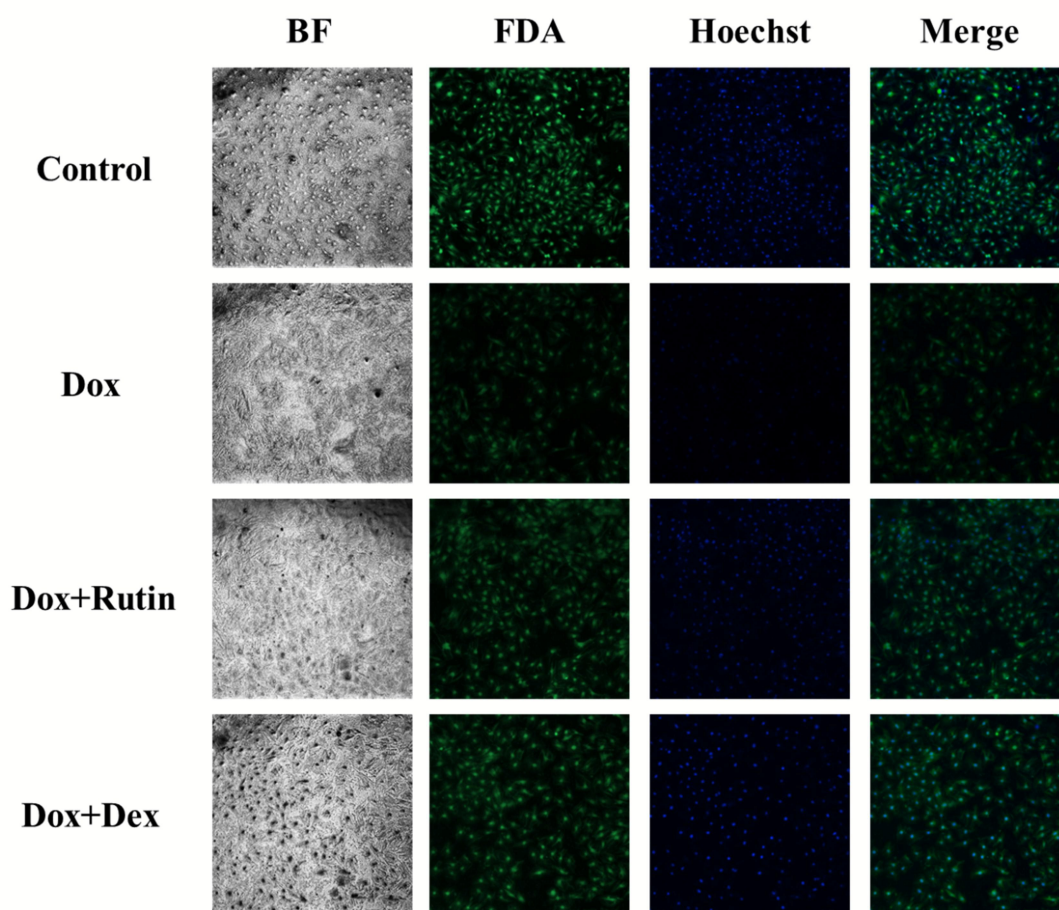


Fig.3 Bright-field and dual fluorescence images of H9c2 by microscope (100 \times) with or without rutin and dexrazoxane pre-incubation.

Rutin dose-dependently attenuated the DOX-induced decrease in the fluorescence intensity of FDA and Hoechst. As shown in Fig.S2, the EC₅₀ value of rutin was approximately 104 μM (FDA) and 137 μM (Hoechst). The results indicate that the pre-incubation of rutin with cardiac muscle cells significantly inhibited the damage on cellular membrane and nucleus. This result is consistent with a previous report that rutin exerts cardioprotective effects by inhibiting oxidative stress²³. Therefore, the proposed model is suitable for screening active compounds against DOX-induced cardiotoxicity.

3.3. Application on screening and identification of cardioprotective components from ZQFZ

The proposed approach was applied to screen cardioprotective components from 52 ZQFZ fractions. The primary screening revealed five fractions with significant activity against DOX-induced membrane injury or DNA damage were picked out in the primary screening (Fig.S1). Secondary screening was performed to test the efficacy of five active fractions in a dose-dependent manner. Five active fractions showed moderate protective effects, with EC₅₀ values of 136.3, 166.4, 267.6, 176.5, and 233.6 μg·mL⁻¹ under FDA staining and 299.0, 285.8, 310.4, 342.1, and 415.3 μg·mL⁻¹ under Hoechst staining.

As shown in Fig.S3, active fractions of B5, B6, B19, B20 and B22 were analyzed using liquid chromatography coupled with mass spectrometry (LC-MS) with positive and negative electrospray ionization. Majority of the compounds originated from *Ligustrum lucidum*. Table 1 lists the molecular weight and formula of the identified compounds. A previous study reported that extracts of *L. lucidum* reduce butylated hydroxytoluene-induced oxidative stress by upregulating anti-oxidant enzymes²⁴. However, the cardioprotective effects of compounds from *L. lucidum* were rarely studied. LC-MS results revealed that cimidahurinine, hydroxytyrosol, and several glucosides such as salidroside, jaspolyside, and neonuezhenide might contribute to the protective effects of active fractions.

PE AK No.	t_R (min)	Identification	Molecular Formula	Ion Mode	[M-H] ⁻ / [M+H] ⁺		Source
					Detected	Error(pp m)	
1	8.88	adenosine	C ₁₀ H ₁₃ N ₅ O ₄	+	268.1043	1.0	<i>Astragalus membranaceus</i> (Fisch.) Bunge.
2	13.66	markhamioside F	C ₁₈ H ₂₆ O ₁₂	-	433.0992	-2.1	Unknown
3	14.70		C ₁₃ H ₁₈ N ₂ O ₈	-	311.0889	1.4	
4	15.37	hydroxytyrosolglucoside	C ₁₄ H ₂₀ O ₈	-	315.1093	2.4	<i>Ligustrum lucidum</i>
5	15.81	cimidahurinine	C ₁₄ H ₂₀ O ₈	-	315.1093	2.4	<i>Ligustrum lucidum</i>
6	15.88		C ₁₄ H ₁₈ O ₈	-	313.0934	1.6	
7	16.25	hydroxytyrosol	C ₈ H ₁₀ O ₃	-	153.0557	8.4	<i>Ligustrum lucidum</i>
8	18.59	salidroside	C ₁₄ H ₂₀ O ₇	+	301.1549	0.5	<i>Ligustrum lucidum</i>
9	31.67	jaspolside	C ₁₇ H ₂₄ O ₁₁	-	403.1246	1	<i>Ligustrum lucidum</i>
10	31.81		C ₂₉ H ₃₆ O ₁₆	-	639.1931	1.6	
11	32.40		C ₃₀ H ₄₀ O ₁₈	-	687.2142	3.2	
12	32.55	6"-O-β-D-glucopyranosyl yleuropein	C ₃₁ H ₄₂ O ₁₈	-	701.2298	3.2	Unknown
13	32.99		C ₃₀ H ₄₀ O ₁₈	-	687.2142	3.4	
14	33.05	angoroside A (-)-isolariciresinol	C ₃₄ H ₄₄ O ₁₉	-	755.2404	3.6	<i>Ligustrum lucidum</i>
15	33.59	3α-O-β-apiofuranosyl-(1->2)-O-β-glucopyranoside	C ₃₁ H ₄₂ O ₁₅	-	653.2451	2	Unknown
16	34.00	3'-hydroxy-4'-methoxy soflavone-7-O-β-D-glucopyranoside	C ₂₂ H ₂₂ O ₁₀	+	447.1291	1.2	<i>Astragalus membranaceus</i> (Fisch.) Bunge.
17	34.41	neonuezhenide	C ₃₁ H ₄₂ O ₁₈	-	701.2298	2.5	<i>Ligustrum lucidum</i>
18	36.39	10-hydroxyyleuropein	C ₂₅ H ₃₂ O ₁₄	-	555.1719	1.9	<i>Ligustrum lucidum</i>
19	37.80		C ₃₀ H ₅₆ O ₂₇	-	847.2914	-2.5	
20	36.69	(8Z)-nuezhenide A	C ₃₁ H ₄₂ O ₁₇	-	685.2349	2.9	<i>Ligustrum lucidum</i>
21	38.61	(8E)-nuezhenide	C ₃₁ H ₄₂ O ₁₇	-	685.2349	2.9	<i>Ligustrum lucidum</i>
22	41.06	(8Z)-nuezhenide	C ₃₁ H ₄₂ O ₁₇	-	685.2349	2.9	<i>Ligustrum lucidum</i>
23	57.34	oleopolynuzhenide A	C ₂₅ H ₂₈ O ₁₂	-	519.1508	1.5	<i>Ligustrum lucidum</i>

Table 1. The HPLC–MS data and identification results of five active fractions.

Hydroxytyrosol, neonuezhenide, salidroside and cimidahurinine were selected and evaluated for their protective activities against DOX-induced cardiotoxicity. All four compounds exerted dose-dependent cardio

protective effects (shown in Fig. 4). The EC_{50} values of hydroxytyrosol, neonuezhenide, salidroside and cimidahurinine were 198.0, 260.4, 621.7, and 45.79 μM under FDA staining. The protective effects calculated by FDA and Hoechst fluorescence differed. FDA staining could monitor membrane permeability and cellular viability, whereas Hoechst 33342 staining reflects DNA damage. The advantage of dual staining approach facilitates the identification of active compounds with different mechanism of action against DOX-induced cardiotoxicity. All identified active compounds exerted protective effects on membrane permeability, suggesting that their efficacies maybe related to preventing oxidative stress-mediated apoptosis.

Salidroside can improve DOX-induced cardiac dysfunction by significantly upregulated the antiapoptotic Bcl2 and downregulated the proapoptotic Bax²⁵. To validate the anti-apoptosis mechanism of active compounds, expression of apoptosis-related proteins were measured in DOX-treated neonatal cardiomyocytes. As shown in Fig.5 (a), hydroxytyrosol, salidroside, cimidahurinine, and neonuezhenide recovered the DOX-induced downregulation of Bcl-2, but only slightly affected Bax. Moreover, intracellular ROS accumulation is regarded as a major mechanism related to DOX induced cardiotoxicity. As shown in Fig.5 (b), DOX was observed to increase intracellular ROS levels in H9c2 cells. After pretreatment of rutin, hydroxytyrosol, neonuezhenide, salidroside, and cimidahurinine, the intracellular concentrations of ROS were significantly decreased. Treatment of DOX (1 μM) for 8 h significantly induced the apoptosis of H9c2 cells when compared to the control. As shown in Fig.5 (c), pretreatment with hydroxytyrosol, neonuezhenide, salidroside, and cimidahurinine significantly decreased the percent of apoptotic cells.

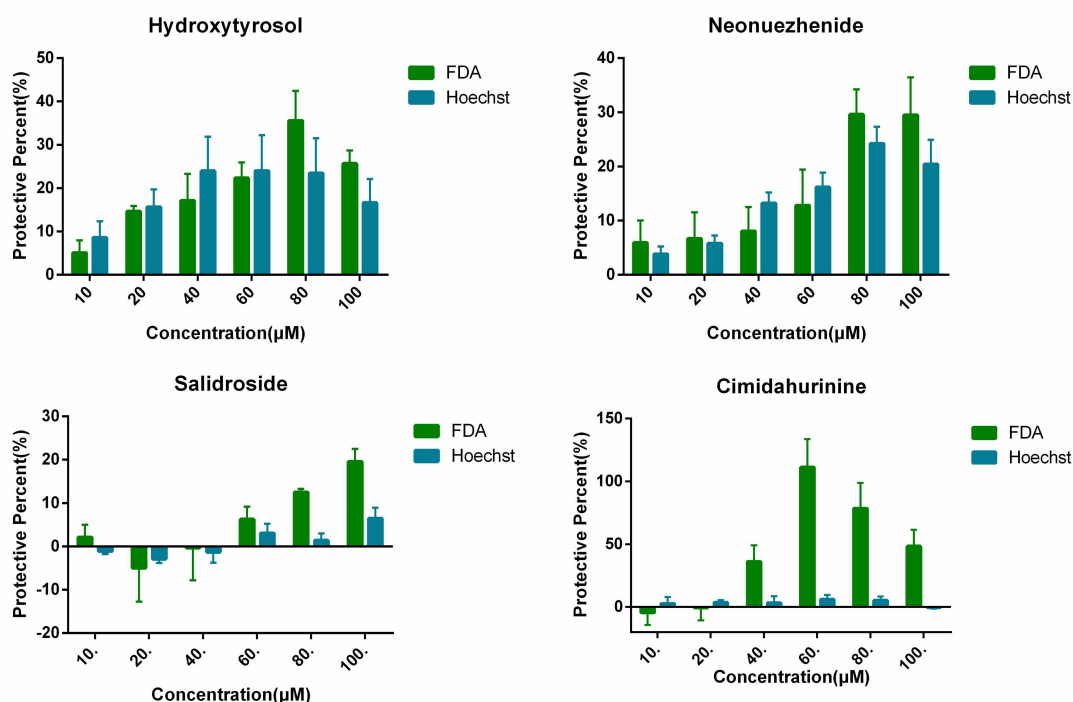


Fig.4 Dose-depend cardioprotection effects on DOX-injured H9c2 cells of four active compounds.

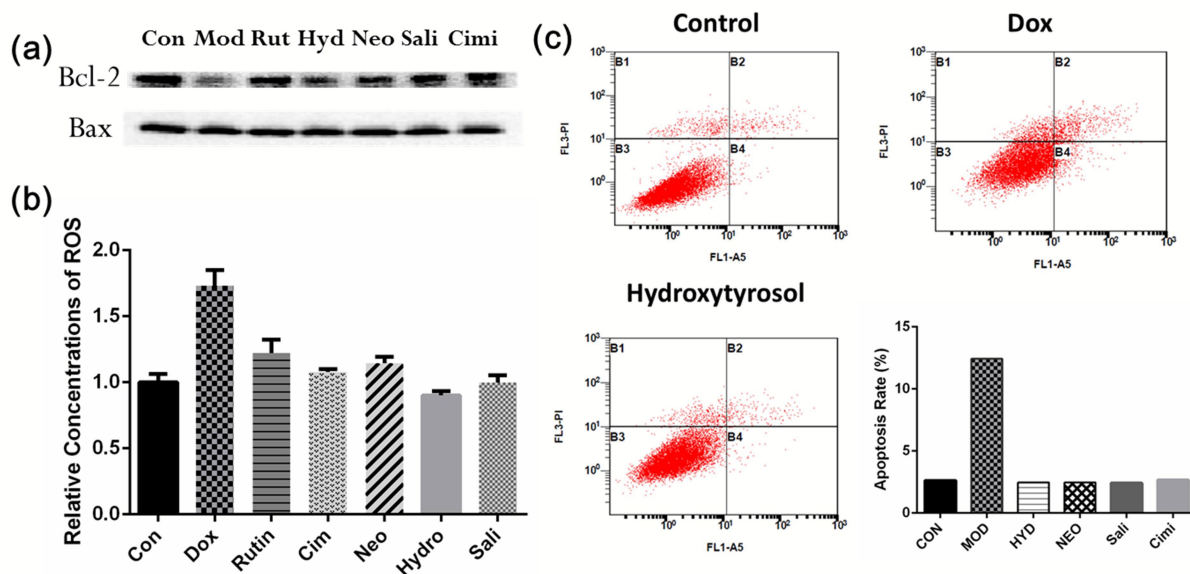


Fig.5 (a) Expression of Bax/Bcl-2 in DOX-treated neonatal cardiomyocytes when pre-protected by Rutin (Rut), hydroxytyrosol (Hyd), salidroside (Sali), cimidahurinine (Cim), and neonuezhenide (Neo). (b). Effects of four active compounds on ROS accumulation in DOX-treated H9c2 cells. (c) Flow cytometry detection of apoptosis with Annexin V/PI. The effect of four active compounds on apoptosis in DOX-injured H9c2 cells.

4. Conclusion

A dual fluorescence imaging technique was developed in this study to detect DOX-induced injury on the membrane and nuclear of cardiac muscle cells. The linear range of the proposed method was from 100 to 10000 in cell number. The proposed method successfully identified four active compounds from ZQFZ. Therefore, the presented approach may offer a rapid technique for screening active compounds against DOX-induced cardiotoxicity from natural products and other complex mixtures.

Acknowledgements

This study was supported by the National Key Scientific and Technological Project of China (No. 2012ZX09304007). The authors would like to acknowledge Dr. Mark Sinnamon in MGH for the help in proofreading of the manuscript.

References

1. B. Neumann, M. Held, U. Liebel, H. Erfle, P. Rogers, R. Pepperkok and J. Ellenberg, *Nat Methods*, 2006, **3**, 385-390.
2. P. Lang, K. Yeow, A. Nichols and A. Scheer, *Nat Rev Drug Discov*, 2006, **5**, 343-356.
3. C. N. Ramirez, T. Ozawa, T. Takagi, C. Antczak, D. Shum, R. Graves, E. C. Holland and H. Djaballah, *Assay Drug Dev Technol*, 2011, **9**, 247-261.
4. P. Ramm, *Curr Opin Biotechnol*, 2005, **16**, 41-48.
5. Y. Wang, X. Zhao, X. Gao, X. Nie, Y. Yang and X. Fan, *Anal Chim Acta*, 2011, **702**, 87-94.
6. Y. Jin, X. Zhao, Y. Zhang, X. Li, X. Nie, Y. Wang and X. Fan, *Int J Toxicol*, 2011, **30**, 287-299.
7. G. Takemura and H. Fujiwara, *Prog Cardiovasc Dis*, 2007, **49**, 330-352.
8. Y. W. Zhang, J. J. Shi, Y. J. Li and L. Wei, *Arch Immunol Ther Ex*, 2009, **57**, 435-445.
9. Y. J. Kang, X. H. Sun, Y. Chen and Z. X. Zhou, *Chemical Research in Toxicology*, 2002, **15**, 1-6.
10. D. Outomuro, D. R. Grana, F. Azzato and J. Milei, *Int J Cardiol*, 2007, **117**, 6-15.
11. A. N. Kavazis, A. J. Smuder, K. Min, N. Tumer and S. K. Powers, *Am J Physiol-Heart C*, 2010, **299**, H1515-H1524.
12. L. P. Solomonson and P. R. Halabrin, *Cancer Research*, 1981, **41**, 570-572.
13. R. G. Eckenhoff and A. P. Somlyo, *Toxicol Appl Pharmacol*, 1989, **97**, 167-172.
14. J. H. Liu, W. K. Mao, B. Ding and C. S. Liang, *Am J Physiol-Heart C*, 2008, **295**, H1956-H1965.
15. Y. Octavia, C. G. Tocchetti, K. L. Gabrielson, S. Janssens, H. J. Crijns and A. L. Moens, *J Mol Cell Cardiol*, 2012, **52**, 1213-1225.
16. Y. Sadzuka, T. Sugiyama, K. Shimoi, N. Kinoshita and S. Hirota, *Toxicol Lett*, 1997, **92**, 1-7.
17. J. Sun, G. Sun, X. Meng, H. Wang, Y. Luo, M. Qin, B. Ma, M. Wang, D. Cai, P. Guo and X. Sun, *PLoS One*, 2013, **8**, e64526.

18. C. Chen and K. Xie, *Practical Journal of Clinical Medicine* 2011, **8**, 89-90.
19. X. Zhao, G. Xu, L. He and L. Ma, *Modern Prevention Medicine*, 2010, **37**, 2759-2764.
20. H. Zhang, H. Geng, X. Jiao, S. Gao and X. Yan, *Shanxi Medical Journal*, 2012, **41**, 475-476.
21. R. Spagnuolo, S. Recalcati, L. Tacchini and G. Cairo, *British journal of pharmacology*, 2011, **163**, 299-312.
22. J. L. Buss and B. B. Hasinoff, *Agents and actions*, 1993, **40**, 86-95.
23. Y. Sadzuka, T. Sugiyama, K. Shimoi, N. Kinae and S. Hirota, *Toxicol Lett*, 1997, **92**, 1-7.
24. H. M. Lin, F. L. Yen, L. T. Ng and C. C. Lin, *J Ethnopharmacol*, 2007, **111**, 129-136.
25. X. L. Wang, X. Wang, L. L. Xiong, Y. Zhu, H. L. Chen, J. X. Chen, X. X. Wang, R. L. Li, Z. Y. Guo, P. Li and W. Jiang, *J Cardiovasc Pharmacol*, 2013, **62**, 512-523.

A dual-fluorescent assay for screening compounds against DOX-induced cardiotoxicity

